

Influence of seepage undercutting on the stability of root-reinforced streambanks

Rachel M. Cancienne,¹ Garey A. Fox^{1*} and Andrew Simon²

¹ Department of Biosystems and Agricultural Engineering, Oklahoma State University, 120 Agricultural Hall, Stillwater, OK 74078, USA

² USDA-ARS National Sedimentation Laboratory, Oxford, MS 38655, USA

*Correspondence to: G. A. Fox, Department of Biosystems and Agricultural Engineering, Oklahoma State University, 120 Agricultural Hall, Stillwater, OK, USA. E-mail: garey.fox@okstate.edu

Abstract

Several mechanisms contribute to streambank failure including fluvial toe undercutting, reduced soil shear strength by increased soil pore-water pressure, and seepage erosion. Recent research has suggested that seepage erosion of noncohesive soil layers undercutting the banks may play an equivalent role in streambank failure to increased soil pore-water pressure. However, this past research has primarily been limited to laboratory studies of non-vegetated banks. The objective of this research was to utilize the Bank Stability and Toe Erosion Model (BSTEM) in order to determine the importance of seepage undercutting relative to bank shear strength, bank angle, soil pore-water pressure, and root reinforcement. The BSTEM simulated two streambanks: Little Topashaw Creek and Goodwin Creek in northern Mississippi. Simulations included three bank angles (70° to 90°), four pore-water pressure distributions (unsaturated, two partially saturated cases, and fully saturated), six distances of undercutting (0 to 40 cm), and 13 different vegetation conditions (root cohesions from 0.0 to 15.0 kPa). A relative sensitivity analysis suggested that BSTEM was approximately three to four times more sensitive to water table position than root cohesion or depth of seepage undercutting. Seepage undercutting becomes a prominent bank failure mechanism on unsaturated to partially saturated streambanks with root reinforcement, even with undercutting distances as small as 20 cm. Consideration of seepage undercutting is less important under conditions of partially to fully saturated soil pore-water conditions. The distance at which instability by undercutting became equivalent to instability by increased soil pore-water pressure decreased as root reinforcement increased, with values typically ranging between 20 and 40 cm at Little Topashaw Creek and between 20 and 55 cm at Goodwin Creek. This research depicts the baseline conditions at which seepage undercutting of vegetated streambanks needs to be considered for bank stability analyses. Copyright © 2008 John Wiley & Sons, Ltd.

Keywords: riparian vegetation; root reinforcement; seepage erosion; soil pore-water pressure; streambank stability

Received 6 September 2007;
Revised 27 November 2007;
Accepted 8 December 2007

Introduction

Sediment is a primary cause of water quality degradation, with the majority of this sediment originating from streambanks in many watersheds. Research has demonstrated that streambank erosion and failure contributes significantly (i.e., up to 80%) to total sediment loading in streams (Bull and Kirkby, 1997; Simon and Darby, 1999; Sekely *et al.*, 2002; Evans *et al.*, 2006). Controlling sediment loading to surface water is important for the protection of human health and freshwater ecosystems; therefore, this sediment loading must be addressed through riparian management strategies.

Several mechanisms can lead to streambank failure and sediment loading to streams, including toe erosion by streamflow undercutting the bank and bank sloughing by removal of matric suction (i.e., generation of positive pore-water pressure) due to precipitation infiltration or stream bank storage. When streambanks are saturated, stability is reduced (Darby and Thorne, 1996; Rinaldi and Casagli, 1999; Simon *et al.*, 2000; Darby *et al.*, 2007). According to Hey *et al.* (1991), bank failures are characterized by either the shape or mode of failure. The Bank Stability and Toe Erosion Model (BSTEM), developed at the USDA-ARS National Sedimentation Laboratory (Simon and Collison, 2002), can simulate both planar and cantilever failures.

Seepage erosion undercutting

One of the processes that initiates mass failure and has received less attention is seepage erosion of non-cohesive sediment by ground-water flow, whereby lateral ground-water emerges from the bank and undercuts the bank by removing soil particles (Fox *et al.*, 2006, 2007a,b; Wilson *et al.*, 2007). Several studies report ground-water sapping, where sapping is defined as the bank collapse resulting from seepage or piping erosion (Laity, 1983; Hagerty, 1991a,b; Worman, 1993; Fox *et al.*, 2007a,b; Wilson *et al.*, 2007). Seepage erosion occurs when high infiltration rates cause perched water tables to develop above water-restricting horizons in riparian soils (Coates, 1990; Wilson *et al.*, 1991; Jones, 1997) or between layers with contrasting hydraulic conductivity (Hagerty, 1991a,b). As perched water tables rise on these less permeable layers, sufficient hydraulic gradients can be generated towards stream channels, causing fairly rapid subsurface flow (interflow) towards streams. This lateral, subsurface flow can potentially result in erosion of unconsolidated material at the outflow face (Higgins, 1982, 1984; McLane, 1984; Dunne, 1990). Seepage flow initiates development and migration of headcuts by liquefaction of soil particles, followed by mass wasting of the stream bank by undercutting, as shown in Figure 1 (Fox *et al.*, 2006, 2007a,b; Wilson *et al.*, 2007). Hagerty (1991a,b) suggest the formation of cavities accelerates the water supply to the exfiltration zone.

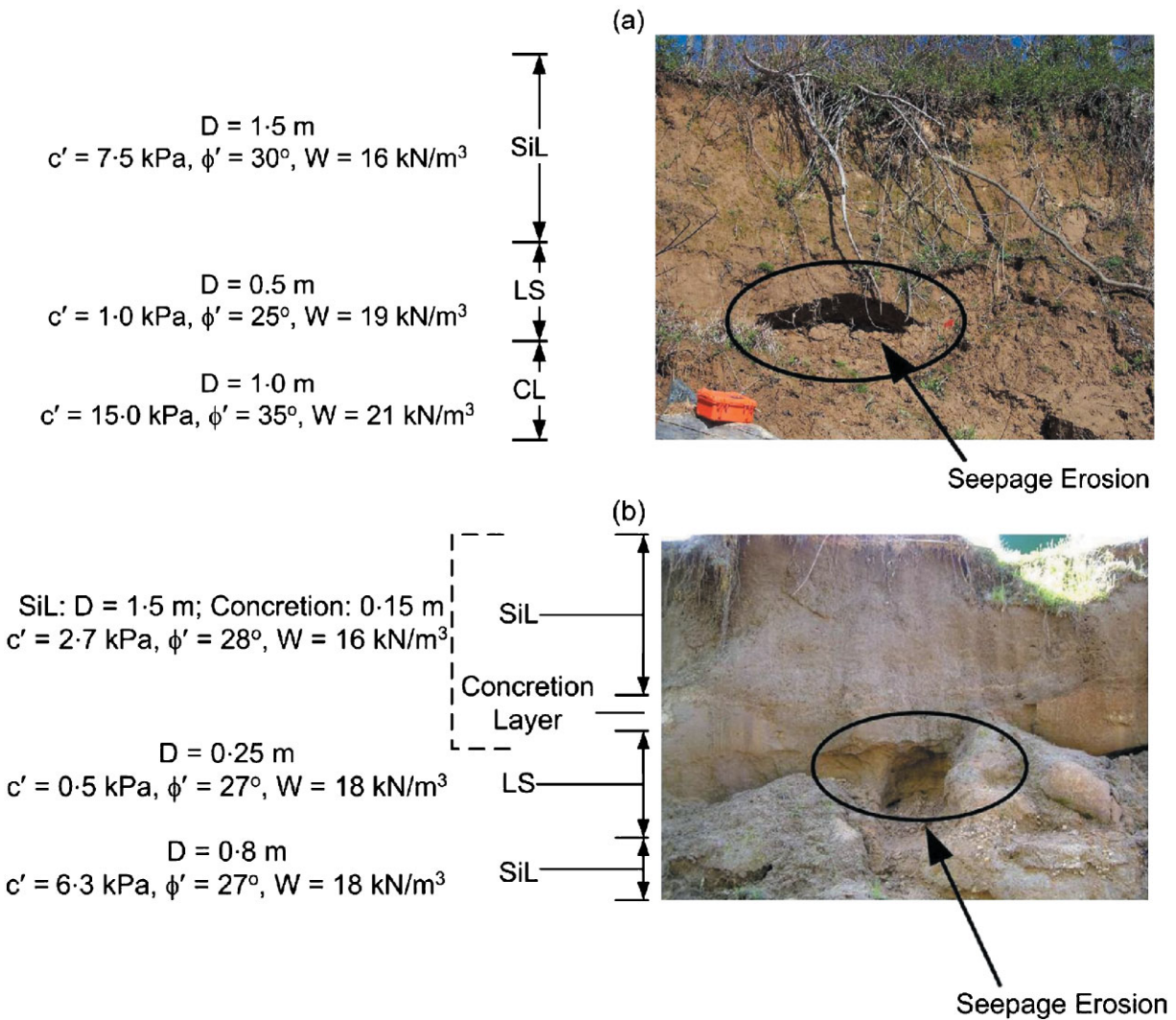


Figure 1. Stratigraphy of the (a) Little Topashaw Creek and (b) Goodwin Creek streambanks simulated using the Bank Stability and Toe Erosion Model. Soil hydraulic and strength parameters are from Langendoen *et al.* (2005), Fox *et al.* (2007a), and Chu-Agor *et al.* (2007). D = depth of streambank layer; c' = effective cohesion; ϕ' = effective angle of internal friction; W = unit weight; SiL = silt loam; LS = loamy sand; CL = clay loam. This figure is available in colour online at www.interscience.wiley.com/journal/esp

Seepage erosion occurs in numerous geographical locations and has been shown to be an important mechanism of streambank failure (Chu-Agor *et al.*, 2007). However, despite this frequent occurrence, little research has been performed regarding the effect of seepage undercutting on bank stability. Additionally, there is little understanding about the importance of seepage undercutting relative to other bank failure mechanisms. Wilson *et al.* (2007) simulated two-dimensional, laboratory lysimeter experiments using the BSTEM by incorporating observed distances of undercutting. Their research indicated that the propensity of streambanks to fail during the recession limb of hydrographs may be the result of interflow-induced seepage erosion undercutting the streambanks, in addition to reduction in the soil shear strength. Chu-Agor *et al.* (2007) and Fox *et al.* (2007b) manually incorporated seepage undercutting into SLOPE/W to account for the interaction between reduced stability by increased pore-water pressure and seepage undercutting. Their work highlighted that the loss of supporting material brought about by seepage undercutting or hydraulic erosion at the bank toe can be a major cause of slope instability and may be of equal or greater importance than the impact of increased soil-water pressure on soil strength. It also highlighted the need to incorporate the dynamic process of seepage erosion into integrated subsurface flow and streambank stability models, but was limited to laboratory conditions, not predictions in the field. Darby *et al.* (2007) have coupled dynamic simulations of bank pore-water pressure with streambank stability models, but not specifically for seepage erosion undercutting.

Root reinforcement

Research has also demonstrated that vegetation plays a role in bank stability, both advantageous and disadvantageous through root reinforcement, surcharge, and hydrological influences, such as soil-water uptake (Wu *et al.*, 1979; Wu, 1984; Thorne, 1990; Beeson and Doyle, 1995; Gray and Sotir, 1996; Micheli and Kirchner, 2002; Simon and Collison, 2002; Pollen *et al.*, 2004; Simon *et al.*, 2006; Zaines *et al.*, 2006; Pollen, 2007). Both field and numerical modelling research has demonstrated that the addition of roots to streambanks improves stability under a range of hydrological conditions (Abernathy and Rutherford, 2000; Wynn *et al.*, 2004; Simon *et al.*, 2006; Pollen, 2007). Small amounts of root reinforcement can provide substantial increases in soil shear strength (Waldron, 1977; Wu *et al.*, 1988a,b; Riestenberg, 1994). Pollen (2007) also noted that root reinforcement increased bank stability over a wide range of soil moisture conditions, but the magnitude varied as a function of soil shear strength and soil moisture content. Wynn and Mostaghimi (2006) discussed the influence of riparian vegetation on subaerial processes of freeze–thaw cycling and soil desiccation.

Objectives

Even with these recent advancements, we still do not understand the *in situ* conditions (i.e., variable soil moisture and vegetation regimes) at which seepage erosion and undercutting needs to be considered in bank stability analyses. In one of the only field studies of undercutting, Simon and Wells (2006) documented through repetitive surveys the amount and timing of erosion of a gully headcut. They demonstrated that mass failure of the gully headwall cannot occur unless the toe of the headcut had been previously undercut by hydraulic erosion or cantilever failures. Fox *et al.* (2007a,b) observed that seepage undercutting distances of only 10 to 30 cm can result in bank collapse at Goodwin Creek. The objective of this research is to utilize the BSTEM to quantify the interrelationship of pore-water pressure, vegetation, and seepage undercutting on bank stability. None of the recent research on bank instability by seepage erosion (i.e., Fox *et al.*, 2006, 2007a,b; Wilson *et al.*, 2007) has investigated root-reinforced streambanks. More specifically, this research addresses two questions. (1) What is the relationship between the factor of safety, FS , water table position (i.e., soil pore-water pressure distribution), and the distance of seepage undercutting as a function of root cohesion? (2) Does the relative importance of undercutting versus increased soil-water pressure depend on root cohesion? Answering these questions will provide guidance as to when the inclusion of seepage undercutting of non-cohesive streambank layers is required in bank stability analyses for river rehabilitation.

Materials and Methods

Streambank stability model

The main purpose of BSTEM is to predict whether or not a streambank will fail by accounting for fluvial undercutting, bank height, bank slope, the unit weight of soil and water in the bank, and surcharge created by objects on top of the bank. The greater resistance a bank has to failure by these forces, the greater its FS . The BSTEM predicts this value by a variety of methods.

As the foundation of BSTEM, Simon *et al.* (2000) utilized the Mohr–Coulomb equation for the shear strength of saturated soil as follows:

$$\tau_f = c' + (\sigma - \mu_w) \tan \phi' \quad (1)$$

where τ_f is the shear stress at failure (kPa), c' is the effective cohesion (kPa), σ is the normal stress (kPa), μ_w is the pore-water pressure (kPa), and ϕ' is the effective angle of internal friction (degrees). In addition, since matric suction (negative pore-water pressure) above the water table increases soil cohesion, the BSTEM defines the shear stress using the following equation from Fredlund and Rahardjo (1993):

$$\tau_f = c' + (\sigma_n - \mu_w) \tan \phi' - (\mu_a + \mu_w) \tan \phi^b \quad (2)$$

where μ_a is the pore-air pressure (kPa), μ_w is the soil pore-water pressure (kPa), and ϕ^b is the rate of increasing soil strength due to increasing matric suction (degrees). The parameter ϕ^b varies between soil types, typically ranging from 10° to 20°, reaching a maximum at ϕ' for saturation (Fredlund and Rahardjo, 1993).

Across horizontal layers, the model uses a limit equilibrium analysis that accounts for up to five user-input soil layers with unique geotechnical properties to calculate the *FS* as follows:

$$FS = \frac{\sum_{i=1}^I c'_i L_i + S_i \tan \phi_i^b + [W_i \cos \beta - U_i + P_i \cos(\alpha - \beta)] \tan \phi'_i}{\sum_{i=1}^I (W_i \sin \beta - P_i \sin[\alpha - \beta])} \quad (3)$$

where c'_i is the effective cohesion of *i*th layer (kPa), L_i is the length of the failure plane of the *i*th layer (m), S_i is the force produced by matric suction on the unsaturated part of the failure surface (kN m^{-1}), W_i is the weight of the *i*th layer (kN), U_i is the hydrostatic-uplift force on the saturated portion of the failure surface (kN m^{-1}), P_i is the hydrostatic-confining force due to external water level (kN m^{-1}), β is the failure-plane angle (degrees from horizontal), α is the bank angle (degrees from horizontal), and I is the number of layers.

Along vertical slices, the model examines the normal and shear forces active in slices of the failure blocks (portions of the bank above the failure surface). This model incorporates a four-step iterative process that includes the normal force acting at the base of a slice, N_j , interslice normal force, I_{nj} , and interslice shear force, I_{sj} , to calculate *FS* using the following equation:

$$FS = \frac{\cos \beta \sum_{j=1}^J (c'_j L_j + S_j \tan \phi_j^b + [N_j - U_j] \tan \phi'_j)}{\sin \beta \sum_{j=1}^J (N_j - P_j)} \quad (4)$$

where J is the total number of vertical slices. For cantilever shear failures, *FS* is merely a ratio of the shear strength of the soil layer(s) to the weight of the cantilever (overhanging soil layer or block):

$$FS = \frac{\sum_{i=1}^I (c'_i L_i + S_i \tan \phi_i^b - U_i \tan \phi'_i)}{\sum_{i=1}^I (W_i - P_i)} \quad (5)$$

Since fibrous roots of vegetation are strong in tension, but weak in compression, their combined effects with soil (which is strong in compression, but weak in tension) create a fairly strong composite material (Wu *et al.*, 1979; Wu, 1984; Thorne, 1990; Gray and Sotir, 1996; Micheli and Kirchner, 2002; Simon and Collison, 2002; Pollen *et al.*, 2004; Simon *et al.*, 2006; Pollen, 2007). Version 4.1 of the model uses the following fiber-break mode, force-equilibrium equation to calculate the increase in soil strength due to root systems:

$$c_r = T_r(A_r/A) (\cos \theta \tan \phi' + \sin \theta) \cong 1.2 T_r(A_r/A) \quad (6)$$

Table I. Types of vegetation and corresponding values of cohesion due to roots, c_r (before application of the vegetation safety margin), and surcharge simulated on the Little Topashaw Creek and Goodwin Creek streambanks with the USDA-ARS Bank Stability and Toe Erosion Model

Cohesion group	Vegetation type	Cohesion (kPa)	Surcharge (kN m ⁻³)
0–5 kPa	Black willow, <i>Salix nigra</i> (5 years)	2.0	0.6
	Sandbar willow, <i>Salix exigua</i> (4 years)	3.0	0.6
	Sweetgum, <i>Liquidambar styraciflua</i> (10 years)	4.0	1.2
5–10 kPa	Himalayan blackberry, <i>Rubus discolor</i> (5 years)	5.5	0.0
	Douglas spirea, <i>Spirea douglasii</i> (3 years)	6.0	0.0
	Gamma grass, <i>Tripsacum dactyloides</i> (5 years)	6.0	0.0
	Longleaf pine, <i>Pinus palustris miller</i> (5 years)	6.0	0.6
	Sycamore, <i>Plantanus occidentalis</i> (7 years)	7.0	0.6
	Eastern cottonwood, <i>Populus deltoides</i> (4 years)	8.0	0.6
	River birch, <i>Betula nigra</i> (7 yrs)	8.0	0.6
> 10 kPa	Alamo switch grass, <i>Panicum virgatum</i> L. (5 years)	18.0	0.0
	Western cottonwood, <i>Populus fremontii</i> (14 years)	30.0	1.2

where c_r is the cohesion due to roots (kPa), T_r is the tensile strength of roots (kPa), A_r/A is the area of shear surface occupied by roots, per unit area (root-area ratio), θ is the shear distortion from vertical (degrees), and ϕ' is the friction angle of soil (Waldron, 1977; Wu *et al.*, 1979; Waldron and Dakessian, 1981). This equation assumes perpendicular orientation of the roots relative to the shear failure plane. Gray and Sotir (1996) and Maher and Gray (1990) note that this assumption is useful because it represents an average of all possible root orientations. The assumption used in BSTEM is that roots of most riparian species are concentrated in the top 1 m of the soil profile (Simon *et al.*, 2007). Therefore, the effects of c_r on stability are equivalent to adding additional c' to the top 1 m of the bank. Pollen and Simon (2005) demonstrated that the above equations overestimate root reinforcement by up to 50% due to neglecting the fact that as the soil-root matrix shears, the roots have different tensile strengths and break progressively. Because of this anticipated 50% overestimation, Version 4.1 of BSTEM includes a vegetation safety margin which allows the user to adjust the maximum root reinforcement predicted by Equation 6 by this factor.

Vegetation also decreases bank stability because of the negative effects of surcharge and increased infiltration into the soil profile. Surcharge increases normal stress due to an increase in mass acting on the surface. It can be calculated by multiplying the mass of the trees by the stocking density on the top of the bank from the De Vries (1974) equation. Default values of c_r and surcharge are provided in the USDA-ARS BSTEM for 12 vegetation species as outlined in Table I. For this research, the vegetation types were divided into three groups based on the estimated c_r after a 50% vegetation safety margin: 0–2.5 kPa, 2.5–5.0 kPa, and greater than 5.0 kPa.

As an additional note on BSTEM, the FS is sensitive to shear surface angles. According to model documentation (Version 4.1), users have two options: (1) vary the shear angle to minimize the FS or (2) use the angle that is the average of the bank angle and the soil friction angle ϕ' . This research minimized the FS by varying the shear angle for each set of experimental conditions and compared the resulting angles with the latter option above. Also, it should be noted that the model does not account for dynamic pore-water pressure variations, shown to be important in triggering mass failures (Darby *et al.*, 2007).

Modelling of field sites

We simulated two streambanks with BSTEM: Little Topashaw Creek and Goodwin Creek in northern Mississippi. Little Topashaw Creek is an incised fourth-order stream near Calhoun City in central Mississippi (Stofleth *et al.*, 2007). Wilson *et al.* (2007) documented the first detailed measurements *in situ* of seepage flow, erosion, and bank undercutting along Little Topashaw Creek. Fox *et al.* (2007a) conducted a similar study at Goodwin Creek, another incised stream which drains a fourth-order, 21 km² northwest Mississippi watershed near Batesville, Mississippi.

The BSTEM was developed to simulate the top 300-cm of the streambank (i.e., above the non-cohesive seepage layer) at Little Topashaw Creek and the top 270-cm of the streambank (i.e., above the seepage layer) at Goodwin Creek with three different bank angles: 70°, 80°, and 90° (Figure 1). A depiction of the stratigraphy, soil hydraulic parameters, soil strength parameters, and model set-up for the Little Topashaw Creek and Goodwin Creek banks is

shown in Figure 1. Soil hydraulic and strength parameters for both sites were derived from Langendoen *et al.* (2005), Fox *et al.* (2007a), and Chu-Agor *et al.* (2007). Banks were simulated with no vegetation ($c_r=0$ kPa and no surcharge) and then with default values for the 12 different vegetation species outlined in Table I. A 50% vegetation safety margin, as suggested by Pollen and Simon (2005), was specified in the model to account for the overestimation of root reinforcement. Confining pressure due to stream stage was neglected; therefore, this research simulated drawdown conditions at low-stream stages representative of conditions on the recession limb of streamflow hydrographs.

Model simulations included various distances (d_u) of hypothetical undercutting within the noncohesive streambank layers: no undercutting ($d_u = 0$ cm), $d_u = 5$ cm, $d_u = 10$ cm, $d_u = 20$ cm, $d_u = 30$ cm, and $d_u = 40$ cm. The shapes of the undercuts used in the simulations were designed to give the smallest *FS* possible. Each undercut formed a triangle such that the elevation of the bottom of the triangle corresponded with the base of the simulated seepage layer (Figure 2). The heights of the triangles were consistent throughout simulations on each bank with the peak at the elevation of the top of the seepage layer. As the distance of undercutting increased with each simulation, the length of the base of the triangular cut increased to the corresponding distance. This mimics the undercut shapes utilized by Chu-Agor *et al.* (2007). The base of the failure surface was placed at the apex of the undercut, as shown in Figure 2.

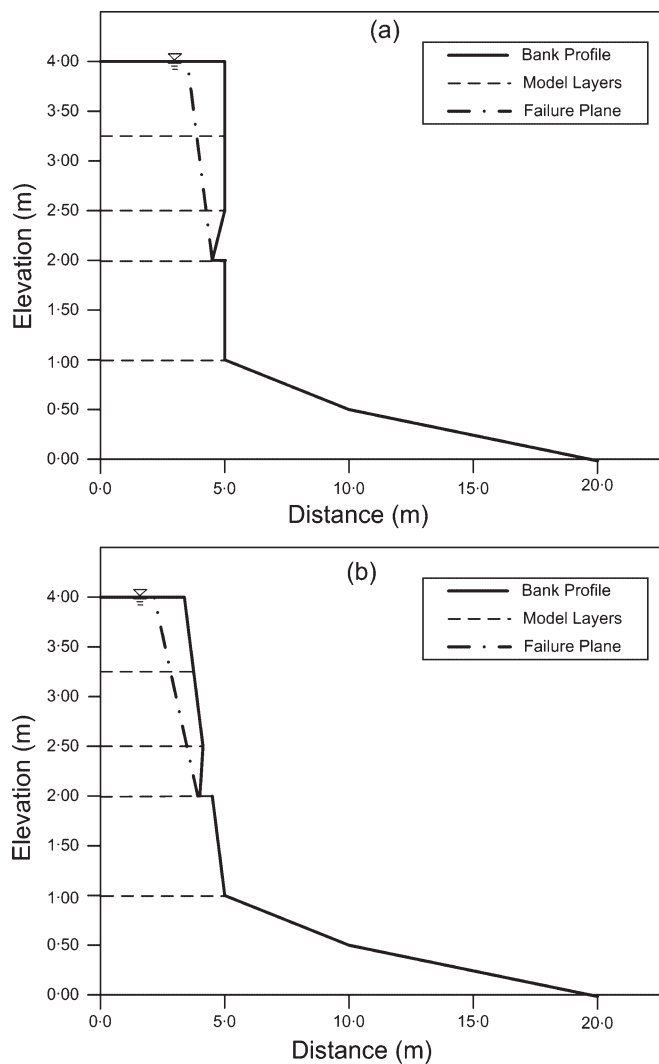


Figure 2. Example Bank Stability and Toe Erosion Model (BSTEM) simulation of Little Topashaw Creek for (a) 90° and (b) 70° banks with undercut distances, $d_u = 40$ cm and fully saturated ground water conditions. This scenario simulates low-stream stage conditions representative of the recession limb of streamflow hydrographs. This figure is available in colour online at www.interscience.wiley.com/journal/esp

To investigate the influence of pore-water pressure on bank stability, we varied the position of the ground-water table relative to the position of the seepage undercut layer. To simulate the influence of negative soil pore-water pressures on the soil shear strength, we used Equation 2 with $\phi^b = 15^\circ$, the default value as suggested by BSTEM. Also, since the typical range reported for ϕ^b is generally between 10° and 20° (Fredlund and Rahardjo, 1993), we used $\phi^b = 15^\circ$ as the midpoint of the expected range. Four different positions of the water table were simulated for each bank: unsaturated, two partially saturated cases, and a fully saturated case. For Little Topashaw Creek, the 0.5-m, non-cohesive seepage undercut layer occurred approximately 1.5 m below ground surface (b.g.s.; Wilson *et al.*, 2007). Therefore, simulations were performed with the ground water table at 2.00 m b.g.s. (unsaturated, 0% of the bank height (BH) where bank height refers to height above the bottom of the seepage layer), 1.50 m b.g.s. (partially saturated, 25% of the BH), 1.00 m b.g.s. (partially saturated, 50% of the BH), and saturated (100% of the BH). For Goodwin Creek, the 0.25-m, non-cohesive seepage undercut layer occurred 1.65 m b.g.s. (Fox *et al.*, 2007a). Simulations included the ground water table at 1.90 m b.g.s. (unsaturated, 0% of the BH), 1.43 m b.g.s. (partially saturated, 27% of the BH), 0.95 m b.g.s. (partially saturated, 50% of the BH), and saturated (100% of the BH). Tension cracks, while known to further reduce the stability of banks, were not included in these simulations. The BSTEM can simulate tension cracks but requires the user to specify the tension crack depth, which for these hypothetical scenarios could only be estimated or assumed. Therefore, the total number of BSTEM simulations was 1872: two banks, three bank angles, four water table positions, six distances of undercutting, and 13 different vegetation conditions.

Analysis of modelling results

The relative sensitivity (S_r) of c_r , d_u , and water table position was calculated based on the following equation:

$$S_r = \left(\frac{\partial O}{\partial P} \right) = \left(\frac{O - O_b}{P - P_b} \right) \left(\frac{P_b}{O_b} \right) \quad (7)$$

where O is the output (i.e., the FS), P is in the input, and the subscript b represents the base value (Byne, 2000). The base line condition for the relative sensitivity analysis was a 70° bank with $c_r = 3.0$ kPa, $d_u = 10$ cm, and WT = 1.50 m b.g.s. for Little Topashaw Creek and WT = 1.43 m b.g.s. for Goodwin Creek. The c_r , d_u , and water table position were varied within the range of -67% to 200% of the original base value.

The next question to be addressed was the relation between the FS and the distance of undercutting for a given c_r value. For both banks, the predicted FS values were first plotted against the ratio of the distance of undercutting and bank height (d_u/BH) above the seepage layer for the various vegetation types with a 50% vegetation safety margin (Table I). As a comparison, similar figures were developed for the relationship between the FS and the height of the water table relative to BH. A critical distance of undercutting (d_u^*) required to reach conditionally unstable conditions (i.e., $FS = 1.3$) was determined based on the $FS - d_u/BH$ plots for each root cohesion value. The d_u^* was non-dimensionalized by the BH and then plotted against the ratio of c_r to the effective cohesion, c' , of each bank. This analysis generated information regarding the d_u^* relative to bank angle, soil pore-water pressure distribution, and root cohesion.

The final question involved the relative importance of undercutting and increased soil-water pressure, investigated in prior research by Fox *et al.* (2006, 2007b), and Wilson *et al.* (2007), in which they suggested that undercutting can possess equivalent or greater importance than increased soil pore-water pressure at some critical distance of undercutting. This research adds another complicating factor in terms of vegetation. The importance of undercutting and soil pore-water pressure at different c_r was determined by calculating the variation in the FS if one of these processes was neglected. More specifically, for each case of bank slope, d_u , water table position, and c_r (e.g., slope = 90° , $d_u = 20$ cm, water table position = 50% of the BH, and $c_r = 8.0$ kPa), the predicted FS was assumed to be the 'true' FS . Two alternative FS values were determined for this scenario by (1) neglecting undercutting (e.g., $d_u = 0$ cm, water table position = 50% of the BH, and all other parameters held constant) and then by (2) neglecting potential rises in the water table position above the seepage layer (e.g., water table position = 0% of the BH, $d_u = 20$ cm, and all other parameters held constant). The error in the FS was calculated between the 'true' FS and the two alternative FS . The alternative FS with the greater error corresponded to the most important process for these conditions (i.e., undercutting versus increased soil pore-water pressure). By considering all possible d_u , water table, and c_r combinations, it was determined whether root cohesion affected the point at which undercutting possessed equal importance to increased soil pore-water pressure. The d_u value for which the error in neglecting undercutting became greater than the error in neglecting soil pore-water pressure effects, referred to hereafter as d_{us} , was determined.

Table II. Predicted factor of safety for Little Topashaw Creek and Goodwin Creek streambanks at various bank angles (α) and distance of undercutting (d_u) as a function of root cohesion (c_r) and water table position. The vegetation safety margin has been applied to c_r . The two FS values under each c_r value are for unsaturated conditions (i.e., water table at the bottom of the seepage layer) and partially saturated conditions (i.e., a water table at 50% of the bank height above the seepage layer), respectively

Stream	α (°)	d_u (cm)	c_r (kPa)			
			0·0	0–2·5	2·5–5·0	> 5·0
Little Topashaw Creek	90	0	1·6, 1·1	1·6, 1·2	1·8, 1·3	2·3, 1·9
		10	1·4, 1·0	1·5, 1·1	1·6, 1·2	2·1, 1·7
		20	1·3, 0·9	1·4, 1·0	1·5, 1·1	1·9, 1·6
		40	1·1, 0·7	1·1, 0·8	1·2, 0·9	1·6, 1·3
	80	0	1·9, 1·4	2·0, 1·4	2·1, 1·6	2·8, 2·2
		10	1·7, 1·2	1·8, 1·3	1·9, 1·5	2·5, 2·0
		20	1·6, 1·1	1·6, 1·2	1·8, 1·3	2·3, 1·9
		40	1·3, 0·9	1·3, 1·0	1·5, 1·1	1·9, 1·5
	70	0	2·3, 1·6	2·4, 1·8	2·6, 2·0	3·4, 2·7
		10	2·1, 1·5	2·2, 1·6	2·4, 1·8	3·1, 2·5
		20	1·9, 1·4	2·0, 1·5	2·2, 1·6	2·8, 2·3
		40	1·6, 1·1	1·7, 1·2	1·8, 1·3	2·4, 1·9
Goodwin Creek	90	0	1·1, 0·6	1·2, 0·7	1·3, 0·9	2·0, 1·5
		10	1·0, 0·5	1·1, 0·6	1·2, 0·8	1·8, 1·4
		20	0·9, 0·5	0·9, 0·6	1·1, 0·7	1·6, 1·2
		40	0·7, 0·4	0·8, 0·4	0·9, 0·6	1·3, 1·0
	80	0	1·3, 0·8	1·4, 0·9	1·6, 1·1	2·4, 1·8
		10	1·2, 0·7	1·3, 0·8	1·5, 1·0	2·1, 1·7
		20	1·1, 0·6	1·2, 0·7	1·3, 0·9	1·9, 1·5
		40	0·8, 0·5	0·9, 0·6	1·1, 0·7	1·6, 1·2
	70	0	1·6, 1·0	1·7, 1·1	1·9, 1·3	2·8, 2·2
		10	1·4, 0·9	1·6, 1·0	1·8, 1·2	2·6, 2·0
		20	1·3, 0·8	1·4, 0·9	1·6, 1·1	2·3, 1·8
		40	1·0, 0·6	1·1, 0·7	1·3, 0·9	1·9, 1·5

Results and Discussion

The predicted FS decreased as α , μ_w , and d_u increased and as the c_r decreased (Table II). The reported increase in the FS relative to addition of roots is equivalent to that reported in other research with BSTEM and other slope stability models (e.g., Abernethy and Rutherford, 2000; Simon *et al.*, 2006; Pollen, 2007). Cohesion due to roots was a more important parameter than surcharge for simulating reinforcement under the conditions modelled. Minimal differences were observed in the predicted FS for vegetation types with the same cohesion but different surcharge (i.e., Douglas spirea, Gamma grass, and longleaf pine). For the Little Topashaw Creek and Goodwin Creek banks, the maximum difference in the predicted FS between the three species listed above was consistently less than 0·10, with these differences decreasing as undercutting increased.

Failure plane angles resulting in the minimum FS were greater at Goodwin Creek as compared with Little Topashaw Creek under similar water table, undercutting, and bank slope conditions because of the lower c' and ϕ' at Goodwin Creek. The shear angles increased as d_u and α increased and decreased as c_r increased (Table III). The data suggest that shear angle is much more sensitive to d_u as compared with c_r and water table position, as the shear angles were independent of water table position. The shear angles resulting in the minimum FS typically bounded the theoretical angle suggested by the average of α and ϕ' .

The S_r analysis for both Little Topashaw Creek and Goodwin Creek banks suggested that the model was most sensitive to water table position (i.e., $S_r = 0·4$ to 0·6). The BSTEM was approximately three to four times more sensitive to water table position than c_r and d_u (Table IV). These results emphasize the importance of appropriately simulating the pore-water pressure distribution for stability analyses as suggested by previous researchers (Darby and Thorne, 1996; Rinaldi and Casagli, 1999; Simon *et al.*, 2000; Darby *et al.*, 2007). The S_r of the model was approximately equivalent (i.e., $S_r = 0·1$ to 0·2) for c_r and d_u at both streambanks (Table IV). Results were similar for other bank angles.

Table III. Shear failure plane angle (degrees) resulting in the minimum factor of safety for Little Topashaw Creek and Goodwin Creek streambanks as a function of bank angle (α), distance of undercutting (d_u), and root cohesion (c_r), and comparison to theoretical shear failure plane angle based on average of α and the internal friction angle (ϕ'). The vegetation safety margin has been applied to c_r .

Stream	α (°)	d_u (cm)	c_r (kPa)				Theoretical ($= \phi' + \alpha$)/2
			0-0	0-2.5	2.5-5.0	> 5.0	
Little Topashaw Creek	90	0	55	55	55	50	60
		10	55	55	55	55	
		20	60	60	60	60	
		40	70	70	70	65	
	80	0	47	47	47	46	55
		10	50	50	50	50	
		20	55	55	55	52	
		40	60	60	60	60	
	70	0	43	42	40	40	50
		10	45	45	45	43	
		20	48	48	48	47	
		40	53	53	53	52	
Goodwin Creek	90	0	60	59	57	53	59
		10	65	63	60	56	
		20	68	65	65	61	
		40	77	75	73	68	
	80	0	52	50	50	47	54
		10	55	55	55	50	
		20	60	59	58	54	
		40	68	67	65	61	
	70	0	45	45	43	41	49
		10	48	48	47	43	
		20	52	52	50	47	
		40	60	60	57	54	

Influence of undercutting and pore-water pressure on stability

The relation between the FS and the d_u/BH ratio was linear to slightly exponential (Figure 3); similar observations were made by Chu-Agor *et al.* (2007) in modelling controlled laboratory experiments of bank instability by undercutting. For a 90° Little Topashaw Creek bank ($c' = 7.5$ kPa in the top 1.5 m of the bank) with no vegetation and unsaturated flow conditions, the bank becomes conditionally unstable with 20 cm of undercutting and unstable (i.e., $FS = 1.0$) with approximately 46 cm of undercutting. The Goodwin Creek bank ($c' = 2.7$ kPa in the top 1.5 m of the bank) with a 90° bank angle was initially conditionally unstable unless the bank possessed vegetation with c_r greater than 2.5 kPa (Figure 3).

Even small degrees of undercutting can counteract the effects of root reinforcement by vegetation with assumed root depths of 1 m. For example, under unsaturated conditions, Little Topashaw Creek or Goodwin Creek 90° vegetated banks with c_r of less than 2.5 kPa were equivalent to a bank without vegetation when the distance of undercutting was approximately 3 to 7 cm on the vegetated bank (Figure 3). For banks with c_r between 2.5 and 5.0 kPa, instability was equivalent to a bank without vegetation when the distance of undercutting was approximately 15 to 20 cm. Such degrees of undercutting are well within the range of maximum observed distances of seepage undercutting in the field (i.e., 10 to 30 cm) as reported by Fox *et al.* (2007a) at Goodwin Creek and Wilson *et al.* (2007) at Little Topashaw Creek.

The FS decreased linearly with increases in the height of the water table relative to the bottom of the seepage layer (Figure 4). These results mimic those of Pollen (2007) in that the effects or impacts of a given magnitude of root reinforcement varied relative to soil shear strength and soil moisture. With a partially saturated bank (i.e., water table at 50% of the BH above the seepage layer), a Little Topashaw Creek or Goodwin Creek bank without vegetation or with c_r less than 2.5 kPa was conditionally unstable without undercutting (Figure 4).

Table IV. Relative sensitivity of BSTEM relative to root cohesion (c_r , kPa), depth of undercutting (d_u , cm) and water table position (WT, m below ground surface, b.g.s.) for Little Topashaw Creek and Goodwin Creek streambanks. The baseline condition for the relative sensitivity analysis was a 70° bank with $c_r = 3.0$ kPa, $d_u = 10$ cm, and WT = 1.50 m b.g.s. for Little Topashaw Creek and WT = 1.43 m b.g.s. for Goodwin Creek

Streambank site	Parameter		Parameter value	Factor of safety (FS)	Relative sensitivity
Little Topashaw Creek	c_r (kPa)	Baseline	3.0	2.08	
		67%	1.0	1.87	0.2
		-50%	1.5	1.91	0.2
		+33%	4.0	2.13	0.1
		+200%	9.0	2.61	0.1
	d_u (cm)	Baseline	10	2.08	
		-50%	5	2.18	-0.1
		+100%	20	1.90	-0.1
		+200%	30	1.73	0.1
	WT (m b.g.s.)	Baseline	1.50	2.08	
		-33%	1.00	1.76	0.5
		+33%	2.00	2.36	0.4
Goodwin Creek	c_r (kPa)	Baseline	3.0	1.46	
		67%	1.0	1.24	0.2
		-50%	1.5	1.29	0.2
		+33%	4.0	1.53	0.1
		+200%	9.0	2.05	0.2
	d_u (cm)	Baseline	10	1.46	
		-50%	5	1.54	0.1
		+100%	20	1.32	0.1
		+200%	30	1.18	-0.1
	WT (m b.g.s.)	Baseline	1.43	1.46	
		-33%	0.95	1.17	0.6
		+33%	1.90	1.74	0.6

Such results suggest that consideration of seepage undercutting is critical for bank stability analyses under unsaturated to partially saturated soil pore-water pressure distributions and is less important under conditions of partially to fully saturated soil pore-water conditions. Saturation conditions result in a reduction in the shear strength of the soil that supersedes the instability due to undercutting investigated in this research. However, seepage flow and undercutting have been reported to occur in the field under unsaturated to partially saturated hydrological regimes (Fox *et al.*, 2007a). In one of the only reported field studies of streambank seepage in conjunction with riparian pore-water pressure measurements, Fox *et al.* (2007a) report over a month of data where seepage flow/undercutting occurred with negative pore-water pressures in the bank material above the seepage horizon.

Critical distance of undercutting for conditionally unstable conditions

For both banks, the critical d_u required to reach conditionally unstable conditions ($FS = 1.3$) with unsaturated pore-water pressures increased logarithmically with c_r/c' , approaching an asymptote with increases in c_r/c' (Figure 5). Greater c_r/c' represents a reinforced bank that requires larger undercutting distances to reduce the FS . The d_u required to reach conditionally unstable banks were approximately 20 cm at Little Topashaw Creek and 0 cm (i.e., no undercutting) at Goodwin Creek for 90° bank angles and approximately 38 cm at Little Topashaw Creek and 2 cm at Goodwin Creek for 80° bank angles without vegetation. For root cohesions of approximately 5.0 kPa, the critical distances of undercutting increased to approximately 35 cm at Little Topashaw Creek and 5 cm at Goodwin Creek for 90° angles and approximately 55 cm at Little Topashaw Creek and 25 cm at Goodwin Creek for 80° angles. Differences between BSTEM predictions for Little Topashaw Creek and Goodwin Creek banks were due to the greater c' and ϕ' , and correspondingly τ_r , at Little Topashaw Creek as compared with Goodwin Creek.

Bank slope appeared to influence the critical distance of undercutting uniformly across the range of c_r investigated (Figure 5). More specifically, the increase in d_u^*/BH was approximately 0.1 with 10° increases in the bank angle. As

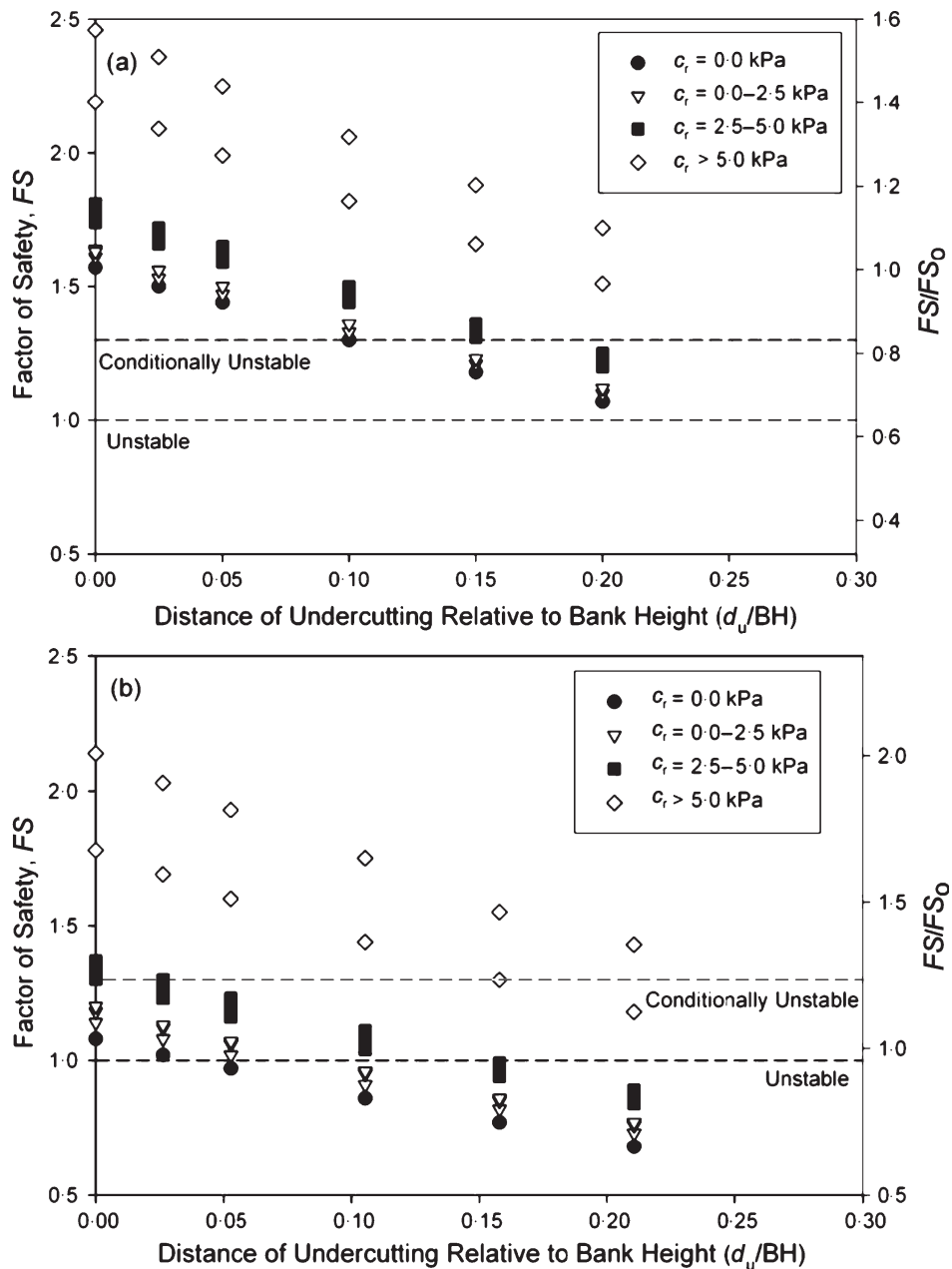


Figure 3. Predicted factor of safety, FS , versus the distance of undercutting (d_u) non-dimensionalized by the bank height above the seepage layer (BH) for various values of root cohesion, c_r , for 90° (a) Little Topashaw Creek and (b) Goodwin Creek banks and for unsaturated soil pore-water pressure conditions (i.e., water table at bottom of the seepage layer). FS_0 refers to the factor of safety for the base condition of no root cohesion (i.e., $c_r = 0.0$ kPa) and no undercutting (i.e., $d_u = 0$ cm). The vegetation safety margin was applied to c_r .

soil pore-water pressure increased (i.e., banks became saturated), the d_u^*/BH decreased for all c_r/c' due to the additional reduced shear strength caused by the increase in μ_w . The influence of water table position on d_u^*/BH was not uniform across c_r . The difference between pore-water pressure curves increased as c_r decreased (Figure 6), suggesting that the interrelationship between water table position and undercutting was more important at lower c_r because of the banks' lower reinforced strength.

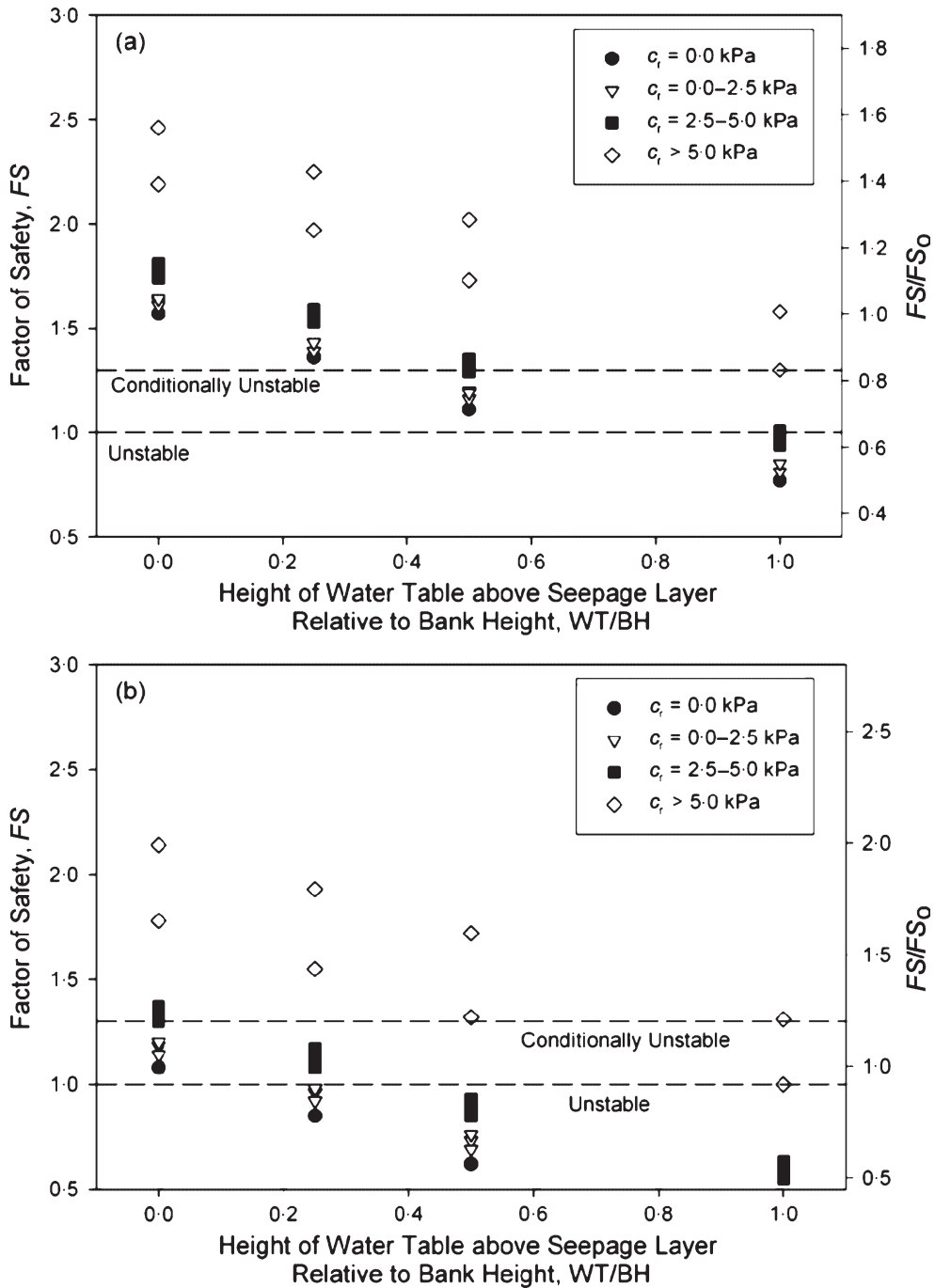


Figure 4. Predicted factor of safety, FS , versus the water table height (WT) non-dimensionalized by the bank height above the seepage layer (BH) for various values of root cohesion, c_r , for 90° (a) Little Topashaw Creek and (b) Goodwin Creek banks and for no undercutting. FS_0 refers to the factor of safety for the base condition of no root cohesion (i.e., $c_r = 0.0$ kPa) and an unsaturated soil profile (i.e., $WT/BH = 0$). The vegetation safety margin was applied to c_r .

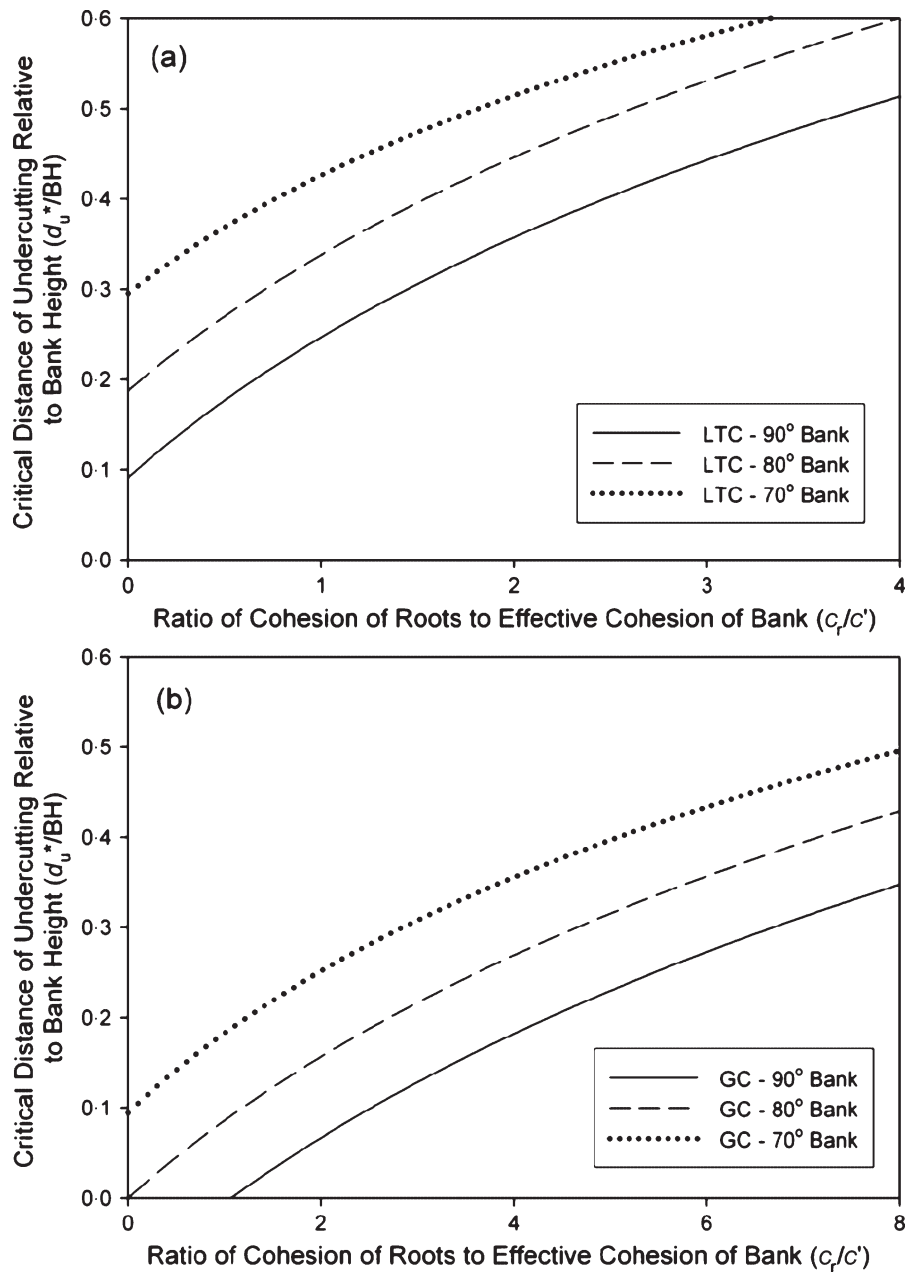


Figure 5. Ratio of critical undercut distance (i.e., distance required to reach conditionally unstable conditions or $FS = 1.3$), d_u^* , relative to cohesion by vegetation for varying bank slopes at (a) Little Topashaw Creek and (b) Goodwin Creek assuming unsaturated conditions (i.e., water table at the bottom of the seepage layer). BH is the bank height above the seepage layer. The vegetation safety margin was applied to c_r .

Instability by undercutting versus soil pore-water pressure

For a specific c_r/c' in Figure 7, the region above each line represents conditions where the undercut geometry (i.e., d_u) is more important than the pore-water pressure (i.e., WT/BH) in determining the FS whereas the region below each line represents conditions where pore-water pressure is more important. The d_{us} appeared independent of bank slope for the conditions modelled (Figure 7a). The d_{us} was greater at Goodwin Creek than Little Topashaw Creek because of

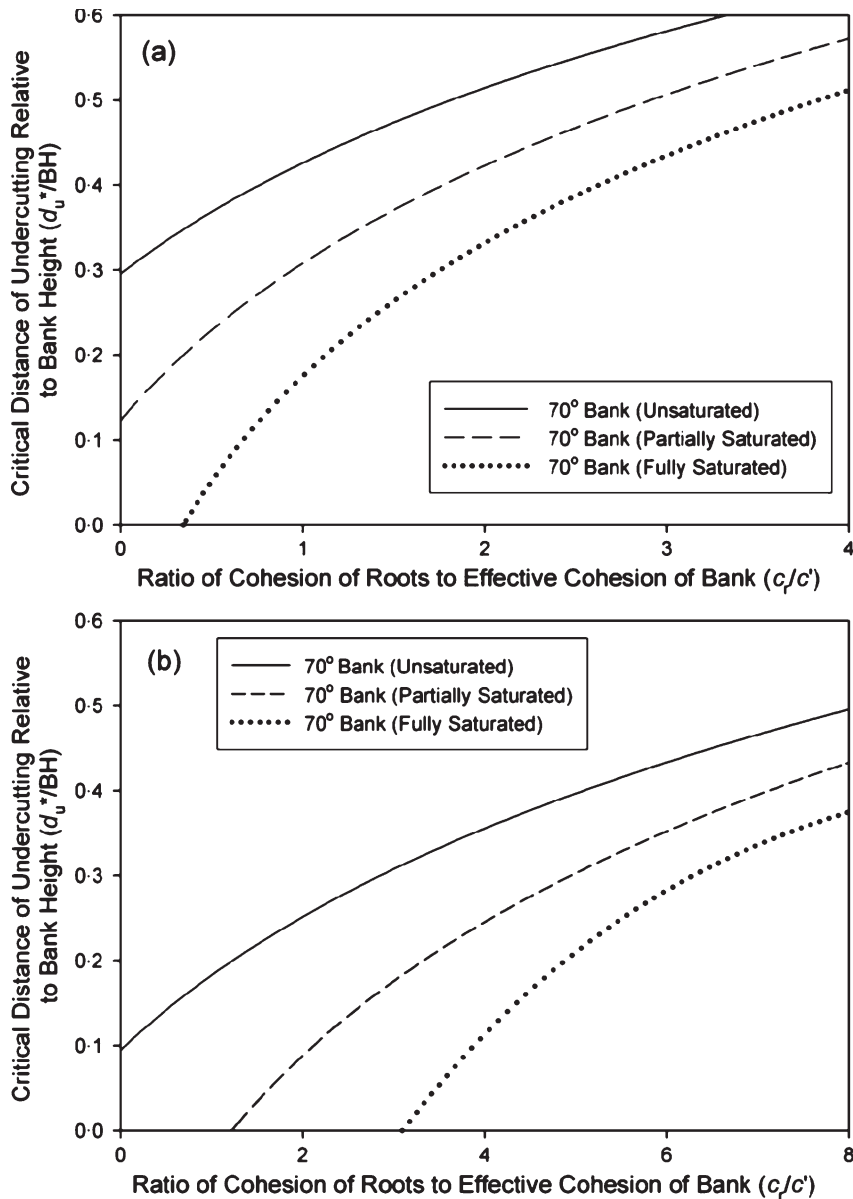


Figure 6. Ratio of critical undercut distance, d_u^* , relative to cohesion by vegetation for varying soil pore-water pressure distributions at (a) Little Topashaw Creek and (b) Goodwin Creek for a 70° bank angle. Unsaturated conditions refer to a bank with a water table at the bottom of the seepage layer. Partially saturated conditions refer to a bank with a water table at 50% of the bank height above the seepage layer (BH). The vegetation safety margin was applied to c_r .

the c' of the banks (Figure 7). Increases in soil pore-water pressure reduced the stability of the less cohesive Goodwin Creek bank ($c' = 2.7$ kPa) more so than the Little Topashaw Creek bank ($c' = 7.5$ kPa).

Consistent among both banks is the fact that undercutting becomes a prominent bank failure mechanism on unsaturated to partially saturated streambanks with greater root reinforcement, even with undercutting distances as small as 20 cm. For Little Topashaw Creek banks under partially saturated conditions (i.e., $WT/BH = 50\%$), neglecting undercutting led to a greater error in the predicted FS when d_{us} was between 20 and 40 cm, with this distance decreasing as c_r increased (Figure 7a). These distances fall well within the range of observed undercutting distances at Little Topashaw Creek (Wilson *et al.*, 2007). For Goodwin Creek banks under similar conditions, the corresponding d_{us} were

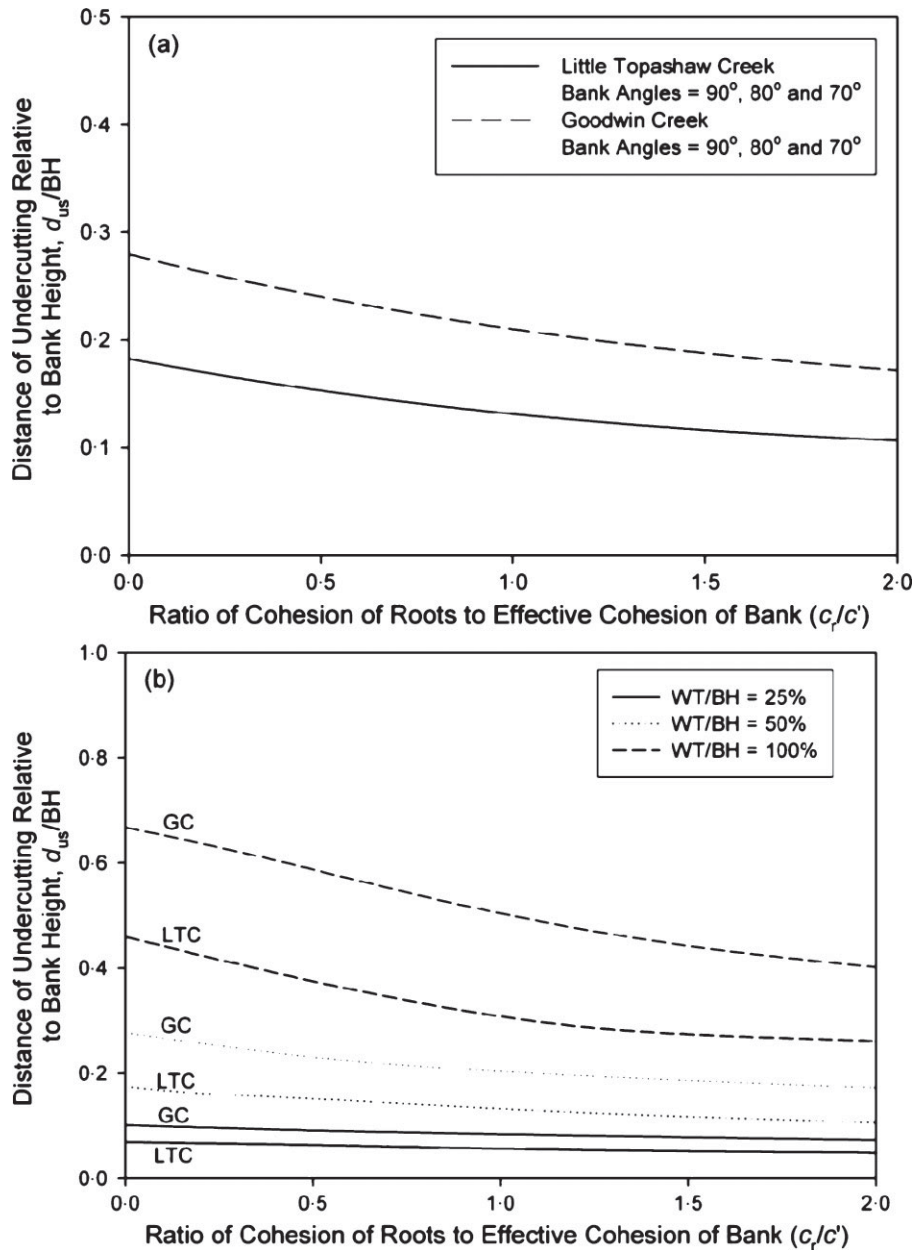


Figure 7. Distance of undercutting, d_{us} , at which the influence of undercutting on stability becomes greater than the influence of soil pore-water pressure relative to root cohesion for (a) various slopes (with water table at 50% of the bank height), and (b) various water table depths for a 80° bank at Little Topashaw Creek and Goodwin Creek. BH is the bank height above the seepage layer. The region above each line represents conditions where the undercut geometry is more important than the pore water pressure whereas the region below each line represents conditions where pore water pressure is more important. The vegetation safety margin was applied to c_r .

less than 20 cm for c_r/c' greater than 5.0 to greater than 55 cm for c_r/c' less than 0.5 (Figure 7b). Under partially saturated conditions with $WT/BH = 25\%$, d_{us} decreased to less than 20 cm for both streambanks. Alternatively, for saturated conditions (i.e., $WT/BH = 100\%$), neglecting pore-water pressure effects resulted in greater errors in the predicted FS for all c_r unless d_{us} approached 100 cm (Figure 7b). Such undercutting distances have not been reported in any field monitoring studies.

Conclusions

As expected, the predicted FS decreased with increasing bank angle, soil pore-water pressure, and distance of undercutting and as root reinforcement decreased for both the Little Topashaw Creek and Goodwin Creek simulated streambanks. The FS decreased linearly or slightly exponentially with increasing distances of undercutting. The FS also decreased linearly with increasing water table elevation relative to the elevation of the base of the seepage layer. The BSTEM was most sensitive to water table position. In fact, the model was approximately three to four times more sensitive to water table position than root cohesion or depth of seepage undercutting, with the BSTEM being equivalently sensitive to these last two parameters. Consideration of the effects of undercutting during unsaturated flow conditions becomes critical for bank stability analyses with very small undercut distances, even with additional cohesion in the top 1.0 m from vegetation; however, these effects become less important under partially to fully saturated soil pore-water conditions because the loss of strength from increased soil pore-water pressure offsets the increase in strength due to c_r . The undercutting distances at which the error in neglecting undercutting became greater than the error in neglecting soil pore-water pressure effects on soil shear strength generally ranged between 20 and 55 cm among the two simulated streambanks and was independent of bank slope. Undercutting tended to be the more prominent bank failure mechanism at smaller distances of undercutting with greater root reinforcement. Due to all of the possible variables involved in streambank stability analyses and cases of river rehabilitation in which young, immature vegetation may be used for root reinforcement, a need exists for streambank stability models that can analyse for site-specific failure processes, including seepage undercutting of non-cohesive streambank layers.

Acknowledgements

This material is based upon work supported by the Cooperative State Research, Education, and Extension Service (CSREES), U.S. Department of Agriculture (USDA), under Award No. 2005-35102-17209. The authors acknowledge Glenn Wilson, USDA-ARS National Sedimentation Laboratory, Oxford, MS, and Amanda Fox, Stillwater, OK for reviewing an earlier version of this manuscript.

References

- Abernethy B, Rutherford ID. 2000. The effect of riparian tree roots on the mass-stability of riverbanks. *Earth Surface Processes and Landforms* **25**(9): 921–937.
- Beeson CE, Doyle PF. 1995. Comparison of bank erosion at vegetated and non-vegetated channel bends. *Water Resources Bulletin* **31**(6): 983–990.
- Bull LJ, Kirkby MJ. 1997. Gully processes and modeling. *Progress in Physical Geography* **21**(3): 354–374.
- Byne WF. 2000. *Predicting sediment detachment and channel scour in the process-based planning model ANSWERS-2000*. ME Thesis. Virginia Tech: Blacksburg, VA.
- Chu-Agor ML, Wilson GV, Fox GA. 2007. *Numerical Modeling of Bank Instability by Groundwater Seepage Flow*. ASABE Paper No. 072117, American Society of Agricultural and Biological Engineers: St Joseph, MI.
- Coates DR. 1990. The relation of subsurface water to downslope movement and failure. In *Groundwater Geomorphology: the Role of Subsurface Water in Earth-surface Processes and Landforms*, Higgins CG, Coates DR (eds). Geological Society of America: Boulder, CO; 51–76.
- Darby SE, Thorne CR. 1996. Numerical simulation of widening and bed deformation of straight sand-bed rivers. I. Model development. *Journal of Hydraulic Engineering* **122**: 184–193.
- Darby SE, Rinaldi M, Dapporto S. 2007. Coupled simulations of fluvial erosion and mass wasting for cohesive river banks. *Journal of Geophysical Research* **112**: F03022. DOI: 10.1029/2006JF000722
- De Vries PG. 1974. Multi-stage line intersect sampling. *Forest Science* **20**(2): 129–133.
- Dunne T. 1990. Hydrology, mechanics, and geomorphic implications of erosion by subsurface flow. In *Groundwater Geomorphology: The Role of Subsurface Water in Earth-Surface Processes and Landforms*, Higgins CG, Coates DR (eds). Geological Society of America: Boulder, CO; 11–28.
- Evans DJ, Gibson CE, Rossell RS. 2006. Sediment loads and sources in heavily modified Irish catchments: A move towards informed management strategies. *Geomorphology* **79**(1–2): 93–113.
- Fox GA, Wilson GV, Periketi R, Cullum RF. 2006. Sediment transport model for seepage erosion of streambank sediment. *Journal of Hydrologic Engineering* **11**(6): 603–611.
- Fox GA, Wilson GV, Simon A, Langendoen E, Akay O, Fuchs JW. 2007a. Measuring streambank erosion due to ground water seepage: Correlation to bank pore water pressure, precipitation, and stream stage. *Earth Surface Processes and Landforms* **32**(10): 1558–1573.
- Fox GA, Chu-Agor M, Wilson GV. 2007b. Erosion of noncohesive sediment by groundwater seepage flow: experiments and numerical modeling. *Soil Science Society of America Journal* **71**(6): 1822–1830.
- Fredlund DG, Rahardjo H. 1993. *Soil Mechanics for Unsaturated Soils*. John Wiley and Sons: New York.

- Gray DH, Sotir RB. 1996. *Biotechnical and Soil Bioengineering Slope Stabilization: A Practical Guide for Erosion Control*. John Wiley and Sons: New York.
- Hagerty DJ. 1991a. Piping/sapping erosion. 1. Basic considerations. *Journal of Hydraulic Engineering* **117**(8): 991–1008.
- Hagerty DJ. 1991b. Piping/sapping erosion. 2. Identification/diagnosis. *Journal of Hydraulic Engineering* **117**(8): 1009–1025.
- Hey RD, Heritage GL, Tovey NK, Boar RR, Grant N, Turner RK. 1991. *Streambank Protection in England and Wales*. R&D Note 22, National Rivers Authority: London; 75 pp.
- Higgins CG. 1982. Drainage systems developed by sapping on Earth and Mars. *Geology Boulder* **10**(3): 147–152.
- Higgins CG. 1984. Piping and sapping: development of landforms by groundwater outflow. In *Groundwater as a Geomorphic Agent*, LaFleur RG (ed.). Allen and Unwin, Inc.: Boston, MA; 18–58.
- Jones JAA. 1997. Subsurface flow and subsurface erosion. In *Process and Form in Geomorphology*, Stoddart DR (ed.). Routledge: London; 74–120.
- Laity JE. 1983. Diagenetic controls on groundwater sapping and valley formation, Colorado Plateau, revealed by optical and electron microscopy. *Physical Geography* **4**: 103–125.
- Langendoen EJ, Lowrance RR, Williams RG, Pollen N, Simon A. 2005. Modeling the impact of riparian buffer systems on bank stability of an incised stream. In *Proceedings of the World Water and Environmental Resources Congress 2004*, 15–19 May, Anchorage AK, Walton R (eds). DOI: 10.1061/40792
- Maher MH, Gray DH. 1990. Static response of sands reinforced with randomly distributed fibers. *Journal of Geotechnical Engineering (ASCE)* **116**(11): 1661–1677.
- McLane CF. 1984. *An experimental and theoretical study of seepage-induced erosion in non-cohesive sediments*. PhD dissertation, University of Virginia.
- Micheli ER, Kirchner JW. 2002. Effects of wet meadow riparian vegetation on streambank erosion: Measurements of vegetated bank strength and consequences for failure mechanics. *Earth Surface Processes and Landforms* **27**(7): 687–697.
- Pollen N. 2007. Temporal and spatial variability in root reinforcement of streambanks: Accounting for soil shear strength and moisture. *Catena* **69**(3): 197–205.
- Pollen N, Simon A. 2005. Estimating the mechanical effects of riparian vegetation on stream bank stability using a fiber bundle model. *Water Resources Research* **41**: W07025. DOI: 10.1029/2004WR003801
- Pollen N, Simon A, Collison A. 2004. Advances in assessing the mechanical and hydrologic effects of riparian vegetation on streambank stability. In *Riparian Vegetation and Fluvial Geomorphology*, Bennett SJ, Simon A (eds). American Geophysical Union: Washington, DC: 125–140.
- Riestenberg MM. 1994. *Anchoring of Thin Colluvium by Roots of Sugar Maple and White Ash on Hillslopes in Cincinnati*. Bulletin 2059-E, U.S. Geological Survey, U.S. Government Printing Office: Washington, DC.
- Rinaldi M, Casagli N. 1999. Stability of streambanks formed in partially saturated soils and effects of negative pore water pressures: the Siene River (Italy). *Geomorphology* **26**: 253–277.
- Sekely AC, Mulla DJ, Bauer DW. 2002. Streambank slumping and its contribution to the phosphorus and suspended sediment loads of the Blue Earth River, Minnesota. *Journal of Soil and Water Conservation* **57**(5): 243–250.
- Simon A, Collison AJC. 2002. Quantifying the mechanical and hydrologic effects of riparian vegetation on streambank stability. *Earth Surface Processes and Landforms* **27**(5): 527–546.
- Simon A, Darby SE. 1999. The nature and significance of incised river channels. In *Incised River Channels: Processes, Forms, Engineering and Management*, Darby SE, Simon A (eds). Wiley: Chichester, UK; 1–18.
- Simon A, Wells RR. 2006. Study of the effects of lateral seepage forces on tension-crack development, bank-failure dimensions and migration of edge of field gullies. In *Proceedings of the 8th Federal Interagency Sedimentation Conference*, 2–6 April, Reno, Nevada.
- Simon A, Curini A, Darby SE, Langendoen EJ. 2000. Bank and near bank processes in an incised channel. *Geomorphology* **35**(3–4): 193–217.
- Simon A, Pollen N, Langendoen E. 2006. Influence of two woody riparian species on critical conditions for streambank stability: Upper Truckee River, California. *Journal of the American Water Resources Association* **42**(1): 99–113.
- Simon A, Pollen N, Jaeger K, Wohl E. 2007. Implications for the Removal of Invasive Species in Canyon de Chelly National Monument. In *Proceedings of the World Water and Environmental Resources Congress 2007*, 15–19 May, Tampa FL, Kabbes KC (ed.).
- Stofleth JM, Shields FD, Fox GA. 2007. Hyporheic and total transient storage in small, sand-bed streams. *Hydrological Processes*. DOI: 10.1002/hyp.6773
- Thorne CR. 1990. Effects of vegetation on riverbank erosion and stability. In *Vegetation and Erosion*, Thornes JB (ed.). Wiley: Chichester, UK; 125–144.
- Waldron LJ. 1977. The shear resistance of root-permeated homogeneous and stratified soil. *Soil Science Society of America Journal* **41**: 843–849.
- Waldron LJ, Dakessian S. 1981. Soil reinforcement by roots: calculation of increased soil shear resistance from root properties. *Soil Science* **132**(6): 427–435.
- Wilson GV, Jardine PM, Luxmore RJ, Zelazny LW, Lietzke DA, Todd DE. 1991. Hydrogeochemical processes controlling subsurface transport from an upper subcatchment of Walker Branch watershed during storm events: 1. Hydrologic transport processes. *Journal of Hydrology* **123**(3–4): 297–316.
- Wilson GV, Periketi RK, Fox GA, Dabney SM, Shields FD, Cullum RF. 2007. Seepage erosion properties contributing to streambank failure. *Earth Surface Processes and Landforms* **32**(3): 447–459.
- Worman A. 1993. Seepage-induced mass-wasting in coarse soil slopes. *Journal of Hydraulic Engineering* **119**(10): 1155–1168.

- Wu TH. 1984. Effect of vegetation on slope stability. *Transportation Research Record* **965**: 37–46.
- Wu TH, McKinnell WP, Swanston DN. 1979. Strength of tree roots and landslides in Prince of Wales Island, Alaska. *Canadian Geotechnical Journal* **16**(1): 19–33.
- Wu TH, Macomber RM, Erb RT, Beal PE. 1988a. Study of soil–root interactions. *Journal of Geotechnical Engineering (ASCE)* **114**(GT12): 1351–1375.
- Wu TH, Beal PE, Lan C. 1988b. In-situ shear test of soil-roots systems. *Journal of Geotechnical Engineering (ASCE)* **114**(GT12): 1376–1394.
- Wynn TM, Mostaghimi S. 2006. Effects of riparian vegetation on stream bank subaerial processes in southwestern Virginia, USA. *Earth Surface Processes and Landforms* **31**(4): 399–413.
- Wynn TM, Mostaghimi S, Burger JA, Harpold AA, Henderson MB, Henry LA. 2004. Variation in root density along stream banks. *Journal of Environmental Quality* **33**(6): 2030–2039.
- Zaimes GN, Schultz RC, Isenhardt TM. 2006. Riparian land uses and precipitation influences on stream bank erosion in central Iowa. *Journal of the American Water Resources Association* **42**(1): 83–97.